Chemistry of Metals and Alloys

Chem. Met. Alloys 16 (2023) 1-6
Ivan Franko National University of Lviv
http://publications.lnu.edu.ua/chemetal

Effect of boron oxide on the structure and optical properties of magnesium fluoride

Viktor ZINCHENKO[1]*, Igor MAGUNOV[1], Anton BABENKO[1], Ganna VOLCHAK[1], Serhii KULESHOV[2], Oleksandr IVANENKO[2]

[1] *Department of Chemistry of Functional Inorganic Materials, A.V. Bogatsky Physico-Chemical Institute, National Academy of Sciences of Ukraine, Lustdorfska road 86, 65080 Odesa, Ukraine*
[2] *Department of Electrochemistry and Technology of Inorganic Materials, Vernadsky Institute of General and Inorganic Chemistry, National Academy of Sciences of Ukraine, Akademika Palladina Ave. 32/34, 03142 Kyiv, Ukraine*
** Corresponding author. Tel.: +380-98-7317030; e-mail: vfzinchenko@ukr.net*

Received May 25, 2023; accepted June 29, 2023
https://doi.org/10.30970/cma16.0427

Magnesium fluoride, MgF_2, is a widely used compound in electrical engineering, optoelectronics, *etc*. Materials based on it have high transparency up to the deep (vacuum) ultraviolet range of the spectrum. Their main disadvantage is the presence of oxide impurities, mainly MgO, which appear during heat treatment and prolonged storage in open air due to hydrolysis or incomplete reaction during synthesis. Addition of boron oxide, B_2O_3, is proposed to bind oxide impurities of basic nature into complex compounds such as fluoroborates. The amount of additive was calculated based on the estimated content of MgO impurities in the material. Excess B_2O_3 was washed with ethanol, which was then removed by prolonged heat treatment. The base substance, MgF_2, and reaction products were identified by infrared transmission spectroscopy and X-ray diffraction. The IR transmittance spectra of the original sample clearly show the bands characteristic of MgF_2, and after the addition of the additive, absorption bands characteristic of B–O bonds are detected, the intensity of which decreases when the additive is washed away. The original MgF_2 preparate is single-phase, but the increase in the width of the peaks and their shift indicate a disturbance in the structure. The average size of the MgF_2 crystallites was calculated according to the well-known Scherrer equation, and is in the range of 14–20 nm (average value 18 nm). After heat treatment with the addition of B_2O_3, the width of the reflections decreases significantly, and after subsequent washing and calcination, the diffractogram of the sample reveals the reflections of magnesium fluoborite, $Mg_3(BO_3)F_3$. According to a quantitative analysis by the Rietveld method, its content is about 8.7% by volume. The thickness of the MgO surface layer on the surface of MgF_2-particles was calculated (about 0.068 nm), and confirms the X-ray amorphous nature of the impurity.

Magnesium fluoride / Oxide impurity / Boron oxide / Infrared spectroscopy / X-ray phase analysis

1. Introduction

Metal fluorides, in particular of some alkali and alkaline earth metals, are widely used in optics in the visible, infrared, and ultraviolet spectral ranges. Magnesium fluoride, MgF_2, combines high transparency in the far (vacuum) ultraviolet range with a low (n = 1.38) refractive index. It is currently the most widely used material among opticians for interference coatings on various optical elements [1-4]. It may be mentioned that MgF_2 was the material that was first used in the world by O. Smakula, our compatriot, to obtain a transmissive coating [5]. However, magnesium fluoride, as well as fluorides of other metals used in optics, has some disadvantages, the main one being the presence of oxygen-containing impurities in the material, mainly MgO. The fact is that focusing on the purpose of separating MgF_2 crystallites (there are no solid solutions in the MgF_2–MgO system [6-10]), magnesium oxide easily interacts with evaporator materials (Mo, Ta) during thermal evaporation in vacuum according to the scheme:

$$3MgO + Mo \xrightarrow{T,\,Vac} Mg\uparrow + MoO_3\uparrow \qquad (1)$$

Thermodynamic calculations show that magnesium fluoride is not capable of such interaction. The products of reaction (1), getting into the coating, deteriorate its optical and operational parameters. Oxygen-containing impurities have the same, if not worse, effect on fiber optic materials. To eliminate them, it is proposed to use nonmetal (Cl, Br) fluorides and KrF_2 or XeF_2 [11]. However, both the reagents themselves and the methods based on them can be considered exotic and, moreover, dangerous for Nature and humans. It should be noted that in some cases, composites of the MgF_2-MgO system are used as a material for applying anti-reflective coatings for the IR spectrum [12].

We have previously developed a method for binding an oxide impurity in magnesium fluoride by exchange reactions with additives of metal fluorides (LnF_3, where *Ln* is Sc, Nd, Lu) [13] according to the scheme:

$$MgO + LnF_3 \xrightarrow{T} MgF_2 + LnOF \quad (2)$$

The resulting lanthanide oxofluorides (their presence was detected by XRD) are less prone to chemical interaction with the evaporator material than MgO. One of the materials used as a binding additive, namely ScF_3, was successfully used in a multilayer interference coating of a broadband filter [14]. There have also been attempts to use other compounds to bind the oxide impurity, in particular, lanthanide sulfofluorides of the general formula *Ln*SF, which should react with the impurity according to a slightly different scheme [15]:

$$MgO + 2LnSF \xrightarrow{T} MgF_2 + Ln_2S_2O \quad (3)$$

At the same time, a method has been proposed that combines exchange reactions with redox reactions with the removal of an oxide impurity, or rather oxygen [16]. For this purpose, a mixture of EuF_3 and ZrF_4 was prepared as an additive reacting according to the equation:

$$2MgO + 4EuF_3 + 2ZrF_4 \xrightarrow{T} 2EuMgF_4 + 2EuZrF_6 + O_2\uparrow \quad (4)$$

Thus, the oxide impurity is almost completely removed to form pure fluoride phases. Eventually, during high-temperature heat treatment (over 1000°C), ZrF_4 is volatilized, leaving behind EuF_2, which acts as additional protection for the evaporator. It should be recognized that the use of rather expensive rare earth fluorides is only appropriate in certain cases.

Recently, we have shown the high efficiency of the addition of boron oxide, B_2O_3, for binding the oxide impurity, ZnO in zinc sulfide and the ZnS–Ge system [17], as well as stabilizing Ge(II) in GeO [18,19]. Due to the fact that B_2O_3 is a very accessible substance (mainly in the form of orthoboric acid) and the low molecular weight of the removed compound, it seemed of interest to study the effect of B_2O_3 addition on the properties of fluorides, in particular MgF_2.

2. Experimental methods

The starting material MgF_2 was a product manufactured by New Materials and Technologies (Odesa). Orthoboric acid H_3BO_3 of grade 14–3 (commercially available) was used as starting material for the production of B_2O_3. The samples were heat-treated in a high-temperature tubular (horizontal) furnace RHTC 804–450 (manufactured by Nabertherm, Germany) in a medium of additionally purified argon. The purification system was manufactured by Valco Instruments Co Inc., USA.

The heat treatment was carried out in several stages at temperatures from 250 to 400°C with steps of 50°C and a holding time of 10 minutes at each stage. An indication of the end of the process is the disappearance of water as condensate on the cold parts of the reactor. At the next stage, which also consists of several stages and is carried out at much higher temperatures – up to 1000°C and a small excess pressure of argon, the holding lasts much longer and takes place every 100°C. The indicator at this stage is the complete absence of gas emission. After the heat treatment, the material is cooled to room temperature, the reactor is opened, and the material is removed for analyses. The test material is pre-ground and pressed into tablets. In this work, three samples were prepared: 1) the original MgF_2; 2) material with the addition of B_2O_3 in an amount that should correspond to the binding of 10 mol.% MgO in MgF_2; 3) material washed with ethanol, followed by prolonged calcination of the sample until the volatile boron compounds and ethanol were completely removed. The indicator was the absence of boron in the washing portions of ethanol (greenish flame).

X-ray diffraction (XRD) of the products was performed on a DRON–3M diffractometer with Cu *Kα* radiation using the powder method. XRD images were taken with focusing according to the Bragg-Brentano scheme in the angular range 10-80° with a step of 0.5° and an exposure of 1 s. The current of the X-ray tube anode was 20 mA, the voltage was 30 kV, and the dimensions of the Soler slits were 002/12/025 mm. The error of the device was 0.01%.

To identify the phase composition of the synthesis products, the diffractograms were processed using the computer software “Match! Crystal Impact ver. 3.3” with FullProfs toolbar [20] and the databases “ICDD PDF-2”, and “COD (Crystallography Open Database)”.

The average particle size was calculated using the Scherrer formula:

$$d = \frac{K\lambda}{\beta\cos\theta} \quad (5)$$

where d is the average particle size, nm; K is the dimensionless particle shape factor (Scherrer's constant), which is 0.9; λ is the X-ray wavelength, Å; β is the width at half-height of the X-ray peak, °; θ is the diffraction angle, °.

The Rietveld method and the Jana2020 program [21] were used to quantify the phase content in the sample. The calculations were based on the X-ray data of the crystallographic open access database (COD) [22] for the compounds MgF_2 (ID – 9009075, space group $P4_2/mnm$, crystallographic parameters: a = 4.623 Å, c = 3.052 Å) and $Mg_3(BO_3)F_3$ (ID – 9009572, space group $P6_3/m$, crystallographic parameters: a = 8.827 Å, c = 3.085 Å).

The calculation error did not exceed 2.5%.

Taking into account the ability of B_2O_3 to undergo a glass transition, the primary identification of the samples was carried out by infrared transmission spectroscopy. The spectra of the samples pressed into a CsI matrix (manufactured by the Institute of Single Crystals of the National Academy of Sciences of Ukraine, Kharkiv) according to the standard method with a possible sample-matrix ratio of 1:20, were recorded using a Fourier transform spectrometer Frotier manufactured by Perkin-Elmer (USA). The wavenumber measurement range was in the range of 200-4000 cm^{-1}.

3. Results and discussion

The infrared transmission spectrum of the annealed MgF_2 sample without addition of B_2O_3 contains a broad band consisting of two bands of different widths with peaks at 410 and 456 cm^{-1}, and a much narrower band with maximum absorption at 262 cm^{-1} (Table 1). Obviously, they correspond to the valence and strain vibrations of the Mg–F bonds of the matrix, respectively. A very narrow but weak peak at 3616 cm^{-1} was also detected, corresponding to the valence vibrations of hydroxyl groups (Mg–OH) (Fig. 1).

Rather weak but distinct bands in the range of 880-1100 cm^{-1} most likely reflect the presence of SiO_2 impurities, or magnesium silicates, due to calcination of the sample in quartz glass vessels.

The sharp, albeit weak, peak at 666 cm^{-1} is obviously an indication of strain vibrations in hydroxyl groups. Thus, these data indirectly confirm the presence of an oxygen-containing impurity in MgF_2.

With the addition of B_2O_3 and subsequent calcination, the spectral picture of the sample changed dramatically: of course, the absorption bands corresponding to the valence and strain vibrations of the Mg–F bonds remain, although some changes have occurred (see Fig. 1). Thus, a group of bands and peaks have appeared, especially evident at 1246 and 702 cm^{-1}, as well as several less evident ones superimposed on the MgF_2 bands. These new bands and peaks are undoubtedly associated with valence and strain vibrations of the B–O bonds in the additive. The disappearance of the valence vibration peak in the O–H groups is also characteristic, indicating that the MgO impurity is bound in complex compounds. After ethanol washing of the unbound B_2O_3 compound, the picture described for the previous sample did not change qualitatively. However, the intensity of the bands and peaks decreased significantly (by a factor of ~1.5), and some weak peaks disappeared completely. It is clear that this phenomenon is directly related to the removal of a significant part of B_2O_3, which has not formed any chemical bond with the MgO impurity (see Fig. 1). Instead, the intensity of the bands of valence and, especially, strain vibrations of Mg–F bonds has increased markedly, which is understandable due to the increase in the proportion of MgF_2 after the removal of part of B_2O_3.

Along with the above, structural changes can also be seen in Fig. 2, with only the peaks of the crystalline phase of MgF_2 being visible. The rather high halo level and large width of the peaks are evidence of the nanocrystalline nature of the material, and their shift towards lower values of Bragg angles indicates a deviation of the cell parameters from the standard values. The tetragonal symmetry of the MgF_2 crystals in the three samples was confirmed.

The parameters of the MgF_2 cell that we have refined are presented in Table 2 (standard value in parentheses). The crystal system is tetragonal: a = 4.62485 Å (5.623 Å), c = 3.05165 Å (3.0549 Å), space group $P4_2/mnm$.

Thus, the cell parameter c became slightly smaller than the standard value, which is typical for nanostructured systems. The size of the MgF_2 particles (crystallites) calculated by equation (5) was 14-20 nm (18 nm on the average), *i.e.* they can be classified as nanoparticles. The addition of B_2O_3 to the MgF_2 material results in a change in the aspect of the diffraction spectra, namely, they become “slimmer” with a sharp decrease in width, and the halo also decreases by more than a factor 2. This indicates an increase in the degree of crystallinity of the material with a simultaneous increase in the size of the crystallites and a decrease in their defectiveness. The positions of the diffraction peaks get closer to the table values.

Finally, washing the material with ethanol to eliminate excess B_2O_3, followed by calcination changes the entire diffraction pattern except for the peaks characteristic of MgF_2, and peaks of a complex magnesium fluoroborate crystallizing in the hexagonal crystal system, space group $P6_3/m$, crystallographic parameters: a = 8.827 Å, c = 3.1021 Å. Obviously, it is formed by the reaction:

$$3MgF_2 + 3MgO + B_2O_3 \xrightarrow{T} 2Mg_3(BO_3)F_3 \quad (6)$$

The occurrence of adverse reactions of the additive with the main substance is also not excluded, in particular:

$$3MgF_2 + 2B_2O_3 \xrightarrow{T} Mg_3(BO_3)F_3 + 3BOF\uparrow \quad (7)$$

Table 1 Positions of bands and absorption peaks of the different MgF_2 samples.

Sample	Wavenumber ($\tilde{\nu}$), cm^{-1}
MgF_2	3616 (v.weak) 1092 (v.weak) 1049 (weak) 1008 (weak) 882 (weak) 666 (weak) 456 (v.strong) 410 (medium) 262 (strong)
$MgF_2 + B_2O_3$	3684 (weak) 1246 (v.strong) 1064 (weak) 897 (v.weak) 743 (medium) 668 (v.weak) 473 (v. strong) 410 (strong) 397 (strong) 357 (medium) 261 (strong) 235 (weak) 210 (v.weak)
$MgF_2 + B_2O_3$ washed	3696 (weak) 1266 (strong) 1250 (v.weak) 1063 (v.weak) 744 (medium) 471 (v. strong) 410 (strong) 357 (weak) 262 (strong) 228 (v.weak)

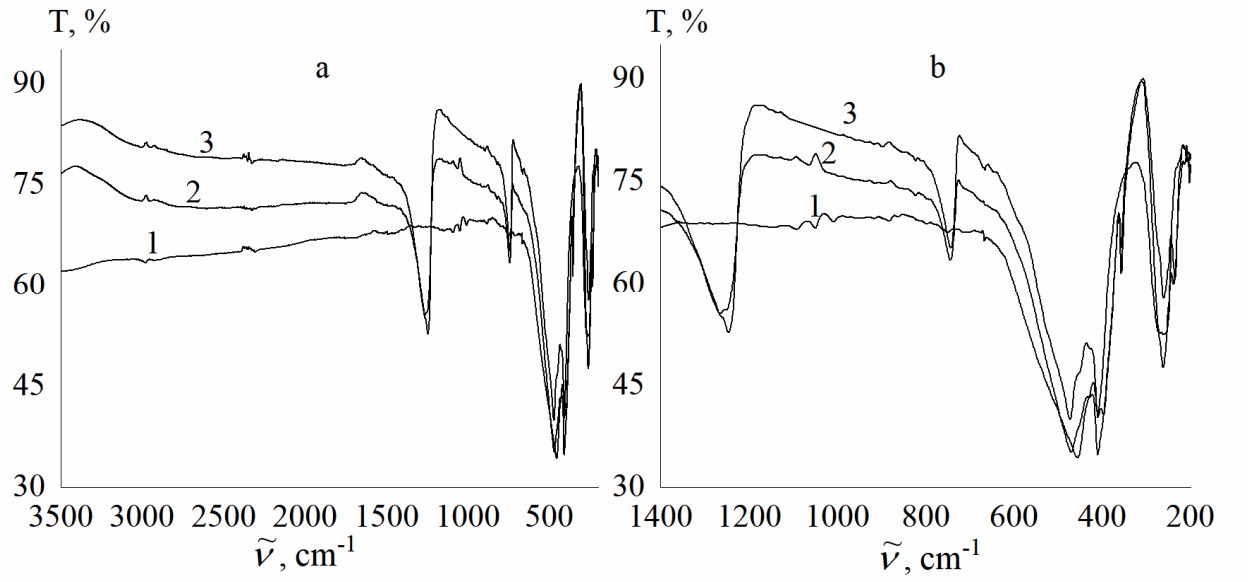

Fig. 1 Infrared transmission spectra in the intervals 3500-200 (a) and 1400-200 (b) cm^{-1} of MgF_2 samples: 1 – original sample, 2 – sample after heat treatment with B_2O_3, 3 – sample after heat treatment with B_2O_3, removal of excess B_2O_3 and repeated heat treatment.

Table 2 Crystallographic parameters of phases in the MgF_2 samples.

Sample	Phase	Symmetry	Space group	Unit-cell parameters, Å
MgF_2	MgF_2, amorph.*	Tetragonal	$P4_2/mnm$	a = 4.6248(5) c = 3.0516(5)
$MgF_2 + B_2O_3$	MgF_2	Tetragonal	$P4_2/mnm$	a = 4.6230 c = 0.0520
$MgF_2 + B_2O_3$ washed	MgF_2	Tetragonal	$P4_2/mnm$	a = 4.6230 c = 3.0520
	$Mg_3(BO_3)F_3$	Hexagonal	$P6_3/m$	a = 8.8602 c = 3.1021

* X-ray amorphous component

Thus, in this case, boron oxide clearly plays the role of a substance that promotes crystallization with the transition from an amorphous to a crystalline substance, as is the case, according to Mao and Lu [23], in the TiO_2–ZrO_2 system. B_2O_3 has a similar effect in the Na_2O–Li_2O–CuO [24] and LiF–B_2O_3 [25] systems. At the same time, a decrease in the B_2O_3 content plays a positive role in this process. The content (vol.%) of MgO in the MgF_2 matrix can be calculated. Using

the Rietveld method, the content of magnesium fluoroborate was initially calculated to be 8.7 vol.%. Hence, the share of MgO is 2.3 vol.%. If we imagine the part of MgF_2 as a sphere with a diameter of 18 nm (radius 9 nm), and MgO as a substance occupying the surface of the MgF_2 particle, then after certain simplifications we obtain the value of d = 0.068 nm = 0.68 Å for the thickness of the MgO layer, which indicates the X-ray amorphous nature of the impurity.

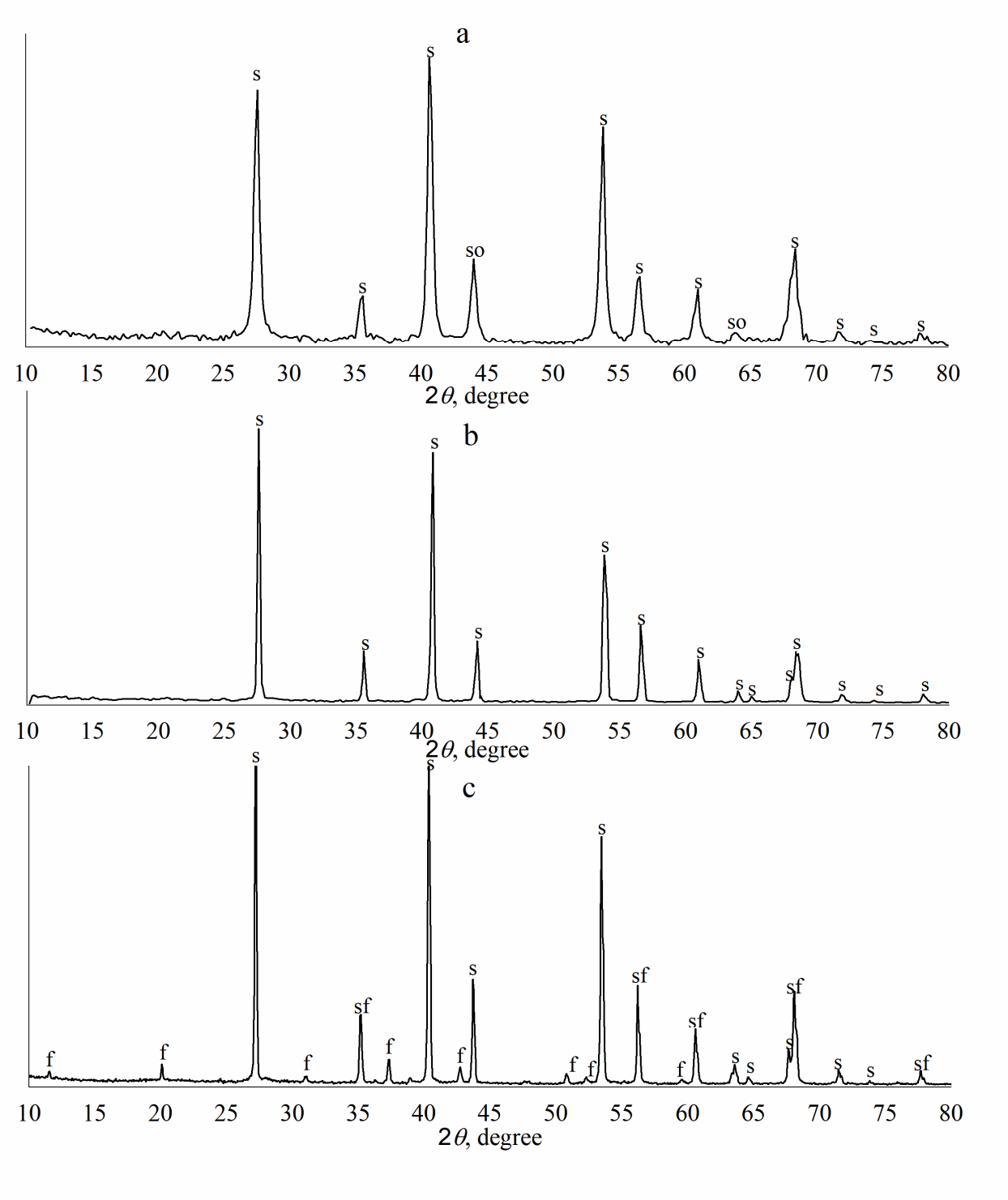

Fig. 2 Diffractograms of MgF_2 samples: a – initial sample, b – sample after heat treatment with B_2O_3, c – sample after heat treatment with B_2O_3, removal of excess B_2O_3 and repeated heat treatment.

Acknowledgement

The authors are grateful to the Head of the Department of Electrochemistry and Technology of Inorganic Materials, Vernadsky Institute of General and Inorganic Chemistry of the National Academy of Sciences of Ukraine, Corresponding Member of the National Academy of Sciences of Ukraine, Doctor of Chemical Sciences, Professor Anatoliy Omelchuk for his assistance in performing structural studies and discussing the results.

References

[1] I.Y. Bubis, V.A. Weidenbach, I.I. Dukhopel *et al.*, *Handbook of the Optical Technologist.* Mashinostroenie, Saint Petersburg, 1983, 414 p.

[2] M.J. Weber, *Handbook of Optical Materials*, CRC Press, Boca Raton, 2002, 536 p. https://doi.org/10.1201/9781315219615

[3] N. Kaiser, H.K. Pulker, *Optical Interference Coatings*, Springer, Berlin, Heidelberg, 2003, 503 p. https://doi.org/10.1007/978-3-540-36386-6

[4] M. Friz, F. Waibel, In: *Springer Ser. Opt. Sci.*, Vol. 88, Springer, Berlin, Heidelberg, 2003, pp. 105-130. https://doi.org/10.1007/978-3-540-36386-6_5

[5] A. Smakula, Patent Deutsches Reich No. 685767. 01.11.1935.

[6] W. Hinz, P.-O. Kunth, *Am. Mineral.* 45 (1960) 1198-1210.

[7] R.A. Sharma, *J. Am. Ceram. Soc.* 71 (1988) 272-276. https://doi.org/10.1111/j.1151-2916.1988.tb05859.x

[8] M. Zielinski, A. Kiderys, M. Pietrowski, I. Tomska-Foralewska, M. Wojciechowska, *Catal. Commun.* 76 (2016) 54-57. https://doi.org/10.1016/j.catcom.2015.12.021

[9] M. Zielinski, B. Czajka, M. Pietrowski, I. Tomska-Foralewska, E. Alwin, M. Kot, M. Wojciechowska, *J. Sol-Gel Sci. Technol.* 84 (2017) 368-374. https://doi.org/10.1007/s10971-017-4495-8

[10] S. Baek, I.-H. Jung, *J. Eur. Ceram. Soc.* 43 (2023) 1723-1734. https://doi.org/10.1016/j.jeurceramsoc.2022.11.027

[11] M.N. Brekhovskikh, V.A. Fedorov, *Inorg. Mater.* 50 (2014) 1277-1282. https://doi.org/10.1134/s0020168514120036

[12] H. Schreiber, J. Wang, S. Wilkinson, U.S. Patent. Pub. N: US 20212/0307353A1, Dec. 6, 2012.

[13] V. Zinchenko, *J. Fluorine Chem.* 131 (2010) 159-164. https://doi.org/10.1016/j.jfluchem.2009.12.001

[14] G.I. Kocherba, V.F. Zinchenko, O.V. Mozkova, M.I. Lyholit, V.P. Sobol, B.A. Gorshtein, Patent of Ukraine for invention dated 26.08.2008, No. 83874.

[15] V.F. Zinchenko, I.R. Magunov, E.V. Timukhin, Kryvda, *J. Phys. Chem. Solids* 12 (2011) 974-979.

[16] E.V. Timukhin, A.A. Bykov, V.F. Zinchenko, S.B. Meshkova, *Ukr. Khim. Zh.* 77 (2011) 16-20.

[17] V.F. Zinchenko, I.R. Magunov, G.V. Volchak, O.V. Mozkova, G.I. Kocherba, *Mater. Today: Proc.* 62 (2022) 5767-5770. https://doi.org/10.1016/j.matpr.2022.03.477

[18] V.F. Zinchenko, I.R. Magunov, O.V. Mozgova, G.V. Nechyporenko, I.V. Stoyanova, *Phys. Chem. Solid State* 19 (2018) 163-170. https://doi.org/10.15330/pcss.19.2.163-170

[19] V.F. Zinchenko, V.P. Sobol, I.R. Magunov, O.V. Mozgova, *Vopr. Khim. Khim. Tekhnol.* 6 (2018) 29-33. https://doi.org/10.32434/0321-4095-2018-121-6-29-33

[20] H. Putz *Match! Phase identification from powder diffraction. Version 3: manual*, Bonn: Crystal Impact, 2020. 143 p.

[21] V. Petricek, M. Dusek, L. Palatinus, *Crystallographic program Jana*, Institute of Physics, Department of Structure Analysis, Praha, 2020.

[22] N. Day, *Crystallography Open Database*, Department of Chemistry, the University of Cambridge, 2023.

[23] D. Mao, G. Lu, *J. Solid State Chem.* 180 (2007) 484-488. https://doi.org/10.1016/j.jssc.2006.11.009

[24] Al-Mokhtar, M. Khadijah *J. Nanotechnol.* 8 (2020) 45-51. http://dx.doi.org/10.12785/jnam

[25] M.A. Ouis, F.H. ElBatal, M.A. Azooz, H.A. ElBatal, *Mater. Chem. Phys.* 283 (2022) 126006. https://doi.org/10.1016/J.MATCHEMPHYS.2022.126006.